

and yields a good SNR in the eye measurements of milliwatt signals with 25 fJ sampling pulses (4 μ W average power). This small power requirement allows a simpler sampling setup. Finally, the optical bandwidth of the sampling setup is 350 GHz.

© IEE 2003

Electronics Letters Online No: 20030681
DOI: 10.1049/el:20030681

7 May 2003

Inuk Kang and K.F. Dreyer (Bell Laboratories, Lucent Technologies, 101 Crawfords Corner Road, Holmdel, NJ 07733, USA)

E-mail: inukkang@lucent.com

References

- OHYA, H., BANJO, N., YAMADA, N., NOGIWA, S., and YANAGISAWA, Y.: 'Measuring eye diagram of 320 Gbit/s optical signal by optical sampling using passively modelocked fibre laser', *Electron. Lett.*, 2001, **37**, pp. 1541–1542
- LI, J., HANSRYD, J., HEDEKVIST, P.O., ANDREKSON, P.A., and KNUDSEN, S.N.: '300-Gbit/s eye-diagram measurement by optical sampling using fiber-based parametric amplification', *IEEE Photonics Technol. Lett.*, 2001, **13**, pp. 987–989
- SCHMIDT, C., SCHUBERT, C., WATANABE, S., FUTAMI, F., LUDWIG, R., and WEBER, H.G.: '320 Gbit/s all-optical eye diagram sampling using gain-transparent ultrafast-nonlinear interferometer'. Proc. 28th ECOC, Copenhagen, Denmark, 2002, Paper 2.1.3
- SHIRANE, M., HASHIMOTO, Y., YAMADA, H., and YOKOYAMA, H.: 'A compact optical sampling measurement system using mode-locked laser-diode modules', *IEEE Photonics Technol. Lett.*, 2000, **12**, pp. 1537–1539
- KANG, I., and YAN, M.: 'A simple setup for simultaneous optical clock recovery and ultrashort sampling pulse generation', *Electron. Lett.*, 2002, **38**, pp. 1199–1201

WDM pilot tone technique for analogue optical links

J. Basak, R. Sadhwani and B. Jalali

The proposed technique overcomes the dynamic range limitations imposed by the signal-pilot beating in analogue fibre optic links. A spurious free dynamic range improvement of 31.8 dB is demonstrated in an experimental link where a pilot tone is used to control the bias point of a Mach-Zehnder modulator.

Introduction and motivation: Second- and third-order harmonics and intermodulation products limit the dynamic range of analogue links. In externally modulated systems using a Mach-Zehnder modulator (MZM), second-order (IM_2) distortions can be kept at a minimum by ensuring that the modulator operates at the quadrature bias [1]. At this bias, there exist only the third-order (IM_3) distortions the magnitudes of which depend on the RF modulation depths. However, device aging, stress, and other environmental variations cause the modulator to deviate from quadrature bias, leading to a large increase in the second-order distortions. This presents the need for a feedback mechanism to maintain the modulator at quadrature bias.

The widely used bias control technique involves the addition of a low frequency, out of band pilot tone to the signal [2]. A portion of the optical power from the output of the modulator is tapped out, and the second harmonic of the pilot tone is measured. Its magnitude is used as a measure of the bias error in a bias-control feedback loop. The measurement sensitivity (O-E conversion plus RF detection) determines both the minimum tap ratio and the minimum pilot tone modulation depth that must be used. The percentage of the optical power tapped out is typically 1%.

As has been pointed out by Ackerman and Cox, in such links, the third-order intermodulation product between signal and the pilot tone will limit the spurious free dynamic range (SFDR) to a value given by $64/(\pi \cdot m_{PT})^4$, where $m_{PT} = V_{PT}/V_{\pi}$ is the modulation depth of the pilot tone, V_{PT} is the peak voltage of the pilot tone and V_{π} is the half wave voltage [2].

In such links, the photodetected RF output power at the second harmonic of the pilot tone (error signal) is given by:

$$P_{out}(2\omega_{PT}) = \frac{1}{2} \left(\frac{\pi^2}{8} \eta P_D \kappa m_{PT}^2 \right)^2 R_{out} \quad (1)$$

where κ is the optical tap ratio, η is the photodetector responsivity, P_D is the optical power input into the photodetector, and R_{out} is the link output impedance. This relation shows that for a given detection sensitivity (constant P_{out}), if κ is increased, m_{PT} can be reduced, allowing an improvement in SFDR as well. However, in the conventional method, increasing κ would mean a reduction in the actual signal power delivered to the link. In this Letter, we propose a technique for eliminating the limit on SFDR imposed by the pilot-signal intermodulation.

Principle: The WDM technique uses two different wavelengths for the signal transmission and the pilot tone detection. Fig. 1 shows the block diagram for the proposed WDM technique. The wavelengths are multiplexed before the MZM. The output of the modulator is demultiplexed and the entire power from the pilot laser is sent into the feedback loop for distortion detection and subsequent bias control. This implies that κ in (1) increases to 100% which is an increase of 100 times compared to a conventional link, where a 1% tap is used. This allows m_{PT} to be decreased by 10 times, resulting in a 40 dB improvement in SFDR, without sacrificing the transmitted signal power. This reduction in the value of m_{PT} is under the assumption of the same optical power from the pilot laser and the signal laser. Smaller output powers of the pilot laser would result in smaller though still substantial improvement in SFDR.

Experimental investigation: We demonstrate the advantage of the WDM technique for a 1550 nm link using an MZM. A DFB laser (JDSU, CQF938/500) emitting 4.5 mW of power at 1550.5 nm was used along with a lithium-niobate (LN) MZM (SEL, TMZ1.5-2.5). A 1% tap was used for the bias detection purpose, to emulate a link with a conventional pilot-tone bias control.

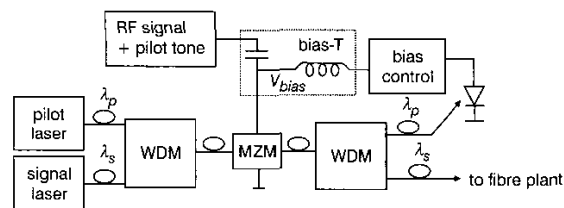


Fig. 1 Schematic diagram of link for WDM technique

For the WDM technique, the same DFB laser was used as the signal laser at 1550.5 nm and another DFB laser (Fujitsu, FLDSF7CZ-J) served as the pilot laser at 1548.1 nm. The optical output power of each laser was adjusted to 4.5 mW at the MZM input, such that the total power is less than the 10 mW maximum input specification of the modulator. The RF signal frequencies were provided by two signal generators (HP8648C/D) at 254 and 255 MHz. A single tone pilot at 1 MHz was provided by a synthesiser (HP3325A).

A spectrum analyser (HP8565E) was used to filter and measure the second harmonic of the pilot tone. The feedback for the bias control was performed using a Labview program, interfacing the spectrum analyser with the variable bias supply (HP6626A). The program sets the MZM bias at the voltage where the second harmonic of the pilot tone is minimised.

The link was shot noise limited, and the output noise floor was measured to be -168.8 dBm/Hz for the conventional technique and -173.4 dBm/Hz for the WDM technique. The difference in the noise floor is due to the optical insertion loss (4.5 dB) of the AWG multi/demultiplexer (NTT) used in the WDM technique. The minimum m_{PT} required for the tapping technique was 1.61% while for the same sensitivity, minimum m_{PT} for the WDM technique was 0.29%. The factor of reduction in m_{PT} (1:6) is less than that calculated (1:10) because of the AWG loss in the WDM technique.

The effect of the m_{PT} reduction in the SFDR is shown in Figs. 2 and 3 where the fundamental and the third-order intermodulation products between signal-signal and signal-pilot are plotted for both the 1% tap

(Fig. 2) and the WDM technique (Fig. 3). Fig. 2 shows the severe limitation of the SFDR due to the signal-pilot IM_3 product. The SFDR in this case was found to be $67.5 \text{ dB-Hz}^{2/3}$, with a degradation of 34.9 dB due to the signal-pilot beating phenomenon. However, using the WDM technique, signal-pilot IM_3 product reduced considerably, resulting in an SFDR of $99.3 \text{ dB-Hz}^{2/3}$, limited only by the signal-signal IM_3 product. Thus, there is an increase of 31.8 dB in the SFDR using the proposed WDM approach.

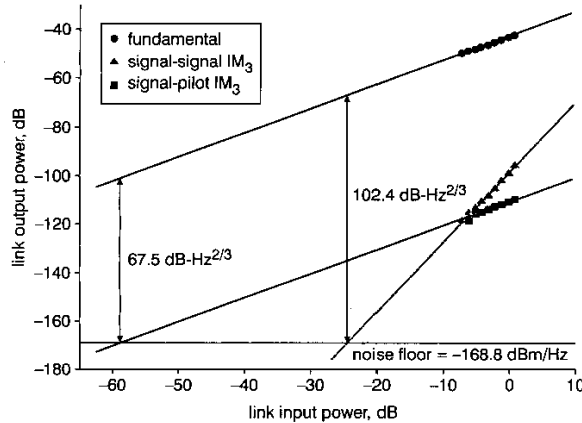


Fig. 2 SFDR plot for conventional bias-control method using 1% tap

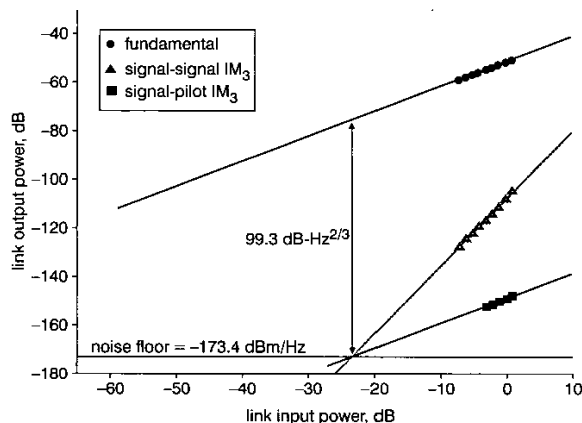


Fig. 3 SFDR plot for WDM pilot tone technique

Discussion: In the proposed system, the measurement and suppression of the distortion is being carried out at the pilot wavelength, which is different from the actual signal wavelength. Because of the dependence of V_π on wavelength, there will be a bias error at the signal wavelength, resulting in finite IM_2 distortion in the link. The wavelength dependence of SFDR in an MZM has recently been studied and quantified [3]. Accordingly, the wavelength dependence of the quadrature bias point is inconsequential as long as the IM_2 distortions do not exceed the IM_3 distortions [3]. For a shot noise limited link, the IM_3 limited SFDR over a bandwidth (B) is given by:

$$SFDR_3 = \left(\frac{2I_{ave}}{qB} \right)^{2/3} \quad (2)$$

In the experiments, the average photocurrent (I_{ave}) was 0.14 mA, suggesting an $SFDR_3$ of $101 \text{ dB-Hz}^{2/3}$, which is in reasonably good agreement with the measured value of $99.3 \text{ dB-Hz}^{2/3}$. Using the results of [3], the allowable signal-pilot wavelength difference ($\Delta\lambda$) for SFDR to be IM_3 limited is given by:

$$\Delta\lambda = \left(\frac{2\sqrt{2}}{\pi} \right) 10^{-(SFDR_3/40)} \cdot \lambda_0 \quad (3)$$

The allowable $\Delta\lambda$ for this value of $SFDR_3$ and $\lambda_0 = 1550 \text{ nm}$ is calculated to be 4 nm, beyond which the link becomes IM_2 limited. A more practical example would be an optical power of 30 mW and a bandwidth of 1 MHz [2]. For such a link, the maximum allowable wavelength spacing would be 20 nm. Such spacing is well within the reach of conventional WDM filters. Since the link will have residual IM_2 distortion, another potential concern is the signal-pilot second-order distortion. However, this distortion would be negligible because its magnitude is proportional to m_{PT} , which is $\ll 1\%$ for the WDM approach.

Conclusion: We have proposed and demonstrated the WDM pilot tone technique for bias control of an MZM. This technique mitigates the limit imposed on SFDR by pilot-signal intermodulation distortion, and ensures that the dynamic range is limited only by the signal-signal distortions. A 31.8 dB improvement of SFDR was demonstrated in an experimental link.

© IEE 2003

Electronics Letters Online No: 20030658

DOI: 10.1049/el:20030658

20 March 2003

J. Basak, R. Sadhwani and B. Jalali (Optoelectronic Circuits and Systems Laboratory, University of California, Los Angeles, CA 90095-1594, USA)

E-mail: juthika@ee.ucla.edu

References

- 1 NAZARATHY, M., BERGER, J., LEY, A.J., LEVI, I.M., and KAGAN, Y.: 'Progress in externally modulated AM CATV transmission systems', *J. Lightwave Technol.*, 1993, 11, (1), pp. 82-105
- 2 ACKERMAN, E.I., and COX, C.H.: 'Effect of pilot tone-based modulator bias control on external modulation link performance'. MWP 2000, Oxford, UK, Paper Tu.4.6
- 3 DUBOVITSKY, S., STEIER, W.H., YEGNANARAYANAN, S., and JALALI, B.: 'Analysis and improvement of Mach-Zehnder modulator linearity performance for chirped and tunable optical carriers', *J. Lightwave Technol.*, 2002, 20, (5), pp. 886-891

High-power InGaAs-on-Si pin RF photodiodes

D.A. Tulchinsky, K.J. Williams, A. Pauchard, M. Bitter, Z. Pan, L. Hodge, S.G. Hummel and Y.H. Lo

High-power InGaAs-on-Si RF pin photodetectors are demonstrated. These diodes dissipate upwards of 640 mW of electrical power, have small-signal compression currents of 91.4 mA at 200 MHz and 71.5 mA at 300 MHz, and dark currents are measured to be less than 10 nA.

Recent advancements in high-speed optical communication systems have focused on increasing the output voltage of photodiodes (PDs) so that logic circuits can be directly driven by the photodetectors, thus eliminating the need for post-detection RF amplifiers [1]. Analogue microwave photonic systems also benefit from improved detectors since high-power/photocurrent PDs increase the dynamic range and reduce the noise figure of externally modulated photonic links [2]. The output power of a photodiode is limited by two factors: (i) space-charge effects – wherein the photogenerated carriers produce a charge screening field that reduces the depletion region electric field to zero, slowing the carrier transport and saturating the optical response [3]; and (ii) ultimately by thermal failure [4-6]. Traditional pin, untravelling carrier (UTC) and dual-depletion-region (DDR) InGaAs PDs grown on lattice-matched InP have been carefully designed to balance the trade-offs between power handling and frequency response of RF photodiodes. These InGaAs/InP photodiode designs are primarily limited thermally by the poor thermal conductivity ($\kappa(300\text{K}) = 0.0475 \text{ W/cm K}$ [7]) of the depleted InGaAs absorber, however a substantial contribution to the thermal impedance can also originate in the InP ($\kappa(300\text{K}) = 0.68 \text{ W/cm K}$ [8]) substrate